LINE MORPHOLOGY INVESTIGATION OF LASER INDUCED GRAPHENE FROM POLYIMIDE FOR 3D PRINTED ELECTRONICS

NICHOLAS CHENG YANG THAM

Singapore Center for 3D Printing, Nanyang Technological University, 50 Nanyang Avenue, Singapore, 639798, Singapore

YOUNG-JIN KIM

Singapore Center for 3D Printing, Nanyang Technological University, 50 Nanyang Avenue, Singapore, 639798, Singapore

VADAKKE MATHAM MURUKESHAN*

Singapore Center for 3D Printing, Nanyang Technological University, 50 Nanyang Avenue, Singapore, 639798, Singapore
**Corresponding author e-mail: mmurukeshan@ntu.edu.sg*

ABSTRACT: First demonstrated in 2014, Direct Laser Writing (DLW) of polyimide (PI) to form Laser Induced Graphene (LIG) is a versatile and simple method to fabricate arbitrary patterns of graphene on PI. LIG can be used to fabricate electrical sensors, biosensors and even energy storage devices that can be integrated in 3D printed circuits and devices. Key to the performance of LIG devices is control over the morphology of the LIG formed, which is still poorly understood. Therefore, this paper will present a preliminary investigation and analysis of the morphology of single LIG lines versus scanning speed and femtosecond (fs) pulse fluence. The results presented will be an important step towards high performance LIG devices.

KEYWORDS: Direct Laser Writing (DLW), Laser Induced Graphene (LIG), Polyimide (PI), 3D Printed Electronics

INTRODUCTION

Ever since the isolation of monolayer graphene, most notably by Novoselov et al. (2004), one of the main goals in graphene research has been to develop a process to quickly and efficiently produce graphene in a form that is directly usable. Graphene is most widely known as a transparent (De & Coleman, 2010), highly conductive allotrope of monolayer carbon (Bolotin et al., 2008), but fabrication of graphene in that form is challenging and is yet to be commercially scalable. More efficient methods of graphene production produce graphene in a wider variety of forms and derivatives, notably graphene with porous 3D structures. Laser Induced Graphene (LIG) from Direct Laser Writing (DLW) of polyimide (PI) or polyimide-based materials is one such process. LIG was first demonstrated in 2014 (Lin et al., 2014) to be an efficient, facile method to quickly produced highly conductive structures of porous graphene. Since then, graphene has found a wide variety of applications in sensing and energy storage (Zhao, Han, Cheng, Jiang, & Qu, 2017). LIG has been found to be induced by a variety of lasers, including fs lasers (In et al., 2015) and in a variety of precursor materials apart from PI (Chyan et al., 2018). The large variety of materials and processes that can form LIG coupled with the ease of arbitrary patterning makes LIG a particularly suitable candidate for integration into laser-based electronics 3D printing processes, such as laser-sintering

Proc. Of the 3rd Intl. Conf. on Progress in Additive Manufacturing (Pro-AM 2018)
Edited by Chee Kai Chua, Wai Yee Yeong, Ming Jen Tan, Erjia Liu and Shu Beng Tor
Copyright © 2018 by Nanyang Technological University
Published by Nanyang Technological University
ISSN: 2424-8967 :: https://doi.org/10.25341/D4101G

of inkjet deposited silver nano-inks, and lithographic processes (Murukeshan, Chua, Tan, & Lin, 2008; Sreekanth & Murukeshan, 2010). Integration of these processes would allow creation of more complex electrical circuits with integrated sensors and energy storage devices (Zhao et al., 2017) or even optical (Sujatha, Murukeshan, Ong, & Seah, 2003) and biosensor systems (James, Murukeshan, & Woh, 2014), which would be a key milestone in the development of 3D printed electronics.

Key to the performance of LIG devices is control over the morphology of the LIG. For example, Duy et al. (2018) found that fibers of LIG grown by rastering a laser beam across PI would enhance the capacitance of micro-supercapacitors by providing a larger area for charge retention near the edge of electrodes. Porous graphene has also been used in electrode arrays for cortical micro-stimulation (Lu, Lyu, Richardson, Lucas, & Kuzum, 2016). Morphological control can be achieved by controlling a whole host of process parameters, such as the writing environment to form super-hydrophobic LIG (Li et al., 2017). Current research is mainly focused on the microstructure of LIG formed, with different microstructures optimized for different applications, such as determining the hierarchal nature of LIG formation for flexible supercapacitors (Andrea et al., 2017). Missing in this research but equally important however, is the spatial distribution of the LIG formed as LIG is written into different materials. The 1D line is the most common building block for DLW LIG devices; arrays of 1D lines are written, or hatched sequentially to form even the most complex of arbitrary shapes. An understanding of how LIG is distributed within a line is therefore critical to control and improve the performance of LIG-based devices. Therefore, results of a preliminary investigation and analysis of the morphology of single LIG lines versus scanning speed and femtosecond (fs) pulse fluence will be presented in this paper. Presentation and further development of these results will be an important step towards improving the performance of large area, multifunctional LIG/3D printed devices.

MATERIALS AND METHODOLOGY

3M Kapton tape was prepared as the sample. A layer of Kapton tape consists of a 30 μm thick layer of PI on a 60 μm thick adhesive layer. To prepare the Kapton sample for writing, the Kapton tape was affixed on a microscope glass slide to provide rigidity and a flat surface for writing. Both the microscope glass slide and the surface of the Kapton tape was cleaned with ethanol to remove organic contaminants. Each line was drawn by scanning a fs laser beam across the sample by means of a computer-controllable galvano-scanner (Sino-Galvo JD2204 Galvo Scanner) fitted with a f-theta lens (Sino-Galvo f-theta lens). The laser used was a linearly polarised Yb-fiber fs laser (Amplitude Systemes Satsuma HP) with a 220 fs pulse duration and 500 kHz repetition rate. The third harmonic wavelength (343 nm) was used for DLW, considering the absorption wavelength of PI. Optical components were installed along the beam line to control the laser parameters under investigation. Power was controlled using a half-wave plate, polarizing beam splitter and beam dump, while a second half-wave plate was used to control the polarization of the beam. The beam was then directed into the galvano-scanner, above an adjustable x-y sample stage as shown in Figure 1.

The surface of the Kapton tape sample was placed at the focus of the galvano-scanner (beam waist measured to be 35 μm across). Each line was 10 mm long, and were drawn at four different scanning speeds, from 50 mms^{-1} to 200 mms^{-1} at 50 mms^{-1} intervals, and at five pulse fluence values from 0.0832 Jcm^{-2} to 0.166 Jcm^{-2}. Each LIG line was drawn twice, and spaced out across the whole sample.

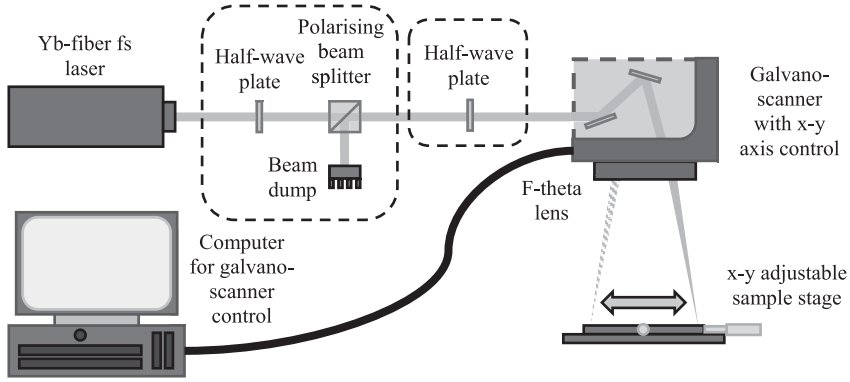

Figure 1. Schematic for DLW of PI with a galvano-scanner.

Raman spectroscopy was conducted with a Renishaw InVia Raman Microscope system. Raman spectra for LIG was excited using a 514 nm laser at 50X magnification. Optical and surface profile characterisation was conducted with a Keyence VK-250 Confocal Microscope at 50X, and surface profiles measured in the software itself.

RESULTS AND DISCUSSION

The formation of glassy carbon on PI by UV irradiation has previously been reported (Schumann, Sauerbrey, & Smayling, 1991), and a variety of carbon-based materials have also been reported from PI such as graphite-like clusters (Nakajima, Nakamura, & Tsuchiya, 2016). Therefore, Raman spectra of each of the lines in which carbonaceous material is observed (under optical microscope) was taken to identify the nature of the carbon-material formed by DLW. Representative spectra was then compared to results of LIG and graphene reported in literature for analysis. The Raman spectra shown in Figure 2 is only representative of the LIG formed in the lines, as different processing parameters investigated can form LIG with differing Raman spectra (Andrea et al., 2017). Across the different Raman spectra, the centre of the D, G and 2D peaks were found at ~1353 cm^{-1}, ~1590 cm^{-1} and ~2700 cm^{-1} respectively. Both the presence and position of 2D peak indicated the formation of graphene (Ferrari et al., 2006). A high D peak indicated high level of disorder, which was expected in the formation of porous LIG (Lin et al., 2014). The wide 2D peak also suggested the formation of many layer graphene (Ferrari et al., 2006), which is also expected of LIG. Since the Raman spectra were in line with what was expected for LIG, therefore it could be safely concluded that LIG was formed.

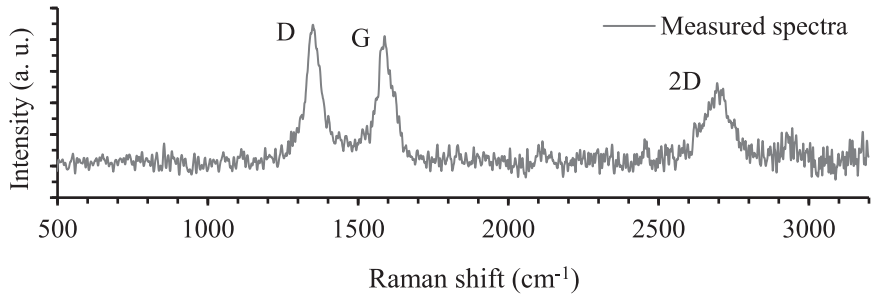

Figure 2. Raman Spectra of LIG formed from DLW of PI. The D peak is at 1353 cm^{-1}, the G peak is at 1591 cm^{-1} and the 2D peak is at 2696 cm^{-1}.

With the formation of LIG confirmed, the next step was to investigate the distribution of LIG across each line. 3D surface profiles of selected sections of the lines were obtained by confocal microscopy, and the results were presented below in Figure 3.

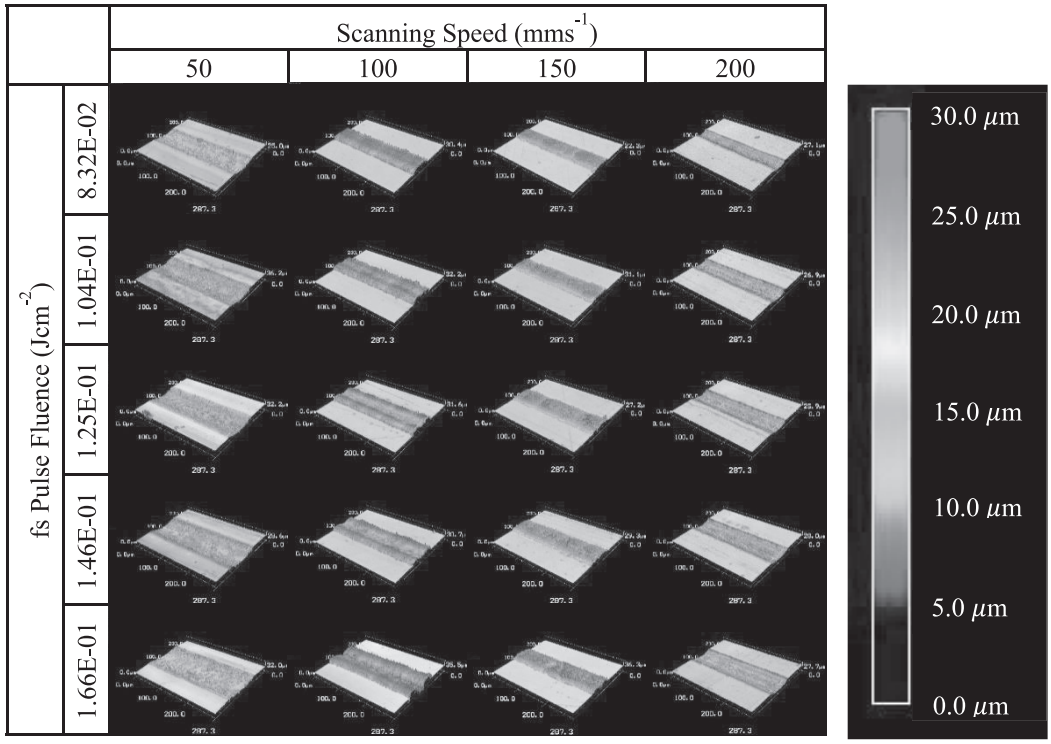

Figure 3. Morphological comparison of LIG line sections with pulse fluence and scanning speed. Colour bar provided to indicate relative heights of LIG and PI.

A few trends can be immediately observed. Firstly, the width of the lines is observed to increase with an increase in pulse fluence. For example at 50 mms^{-1}, the measured line width increased from 78 μm to 110 μm. This positive relationship was found to hold across all other observed speeds as well. Secondly, LIG was only fabricated within a speed range of 100 mms^{-1} to 150 mms^{-1}. Virtually no LIG was observed along the lines at 200 mms^{-1} or 50 mms^{-1}. This result points towards a limited range of scanning speeds to form LIG, beyond which LIG cannot be formed. Thirdly and most importantly, within the acceptable speed range, the distribution of LIG changes drastically. For example at 100 mms^{-1}, the top of the LIG formed a relatively wide (66 μm) and even 'plateau' at 0.0832 Jcm^{-2}, but steadily separated into two thinner lines of LIG separated by a heavily ablated groove in the underlying PI. Such a distribution of LIG has large implications on the quality of larger patterns of LIG formed at these parameters, as it implies that properties of a large LIG pattern might be compromised by the presence of these large gaps. At 150 mms^{-1} (still within range of LIG formation) 'cracks', instead of a full separation within the distributed region of LIG was observed.

The observed distribution of LIG can be explained by the increasing number of pulses with increasing pulse fluence at the same speed. In LDW by pulsed lasers, a written line is simply the cumulative addition of overlapping pulses across the line, with the scanning speed controlling the

amount of overlap of each pulse, resulting in a certain number of pulses per unit length. For example, at 100 mms^{-1}, there are 5,000 pulses per mm (for 500 kHz repetition rate). As pulse fluence increases, the amount of incident pulse energy on the same area increases, and at a particular threshold (experimentally determined to be 0.0416 Jcm^{-2} at 100 mms^{-2}) the formation of LIG due to photo-thermal interaction with the PI occurs (In et al., 2015). Before this threshold (but above the carbonisation threshold), material closer to graphite would be formed instead. The porosity of LIG is a direct result of violent ejection of material (ablation plumes) into the environment (Lin et al., 2014) therefore with a large enough energy intensity (above threshold of 416 Jcm^{-2} this experiment), material ejection from the underlying PI would cause the ejection of the LIG formed above it. Ejection of LIG that would expose the ablated PI layer would be expected to occur at the centre of the line, where the fluence of the beam would be the highest, therefore resulting in the observed 'separated' LIG distribution above 0.0832 Jcm^{-2} at 100mms^{-1}. At 150 mms^{-1} in comparison, the number of pulses per mm would be around 3,333 pulses, therefore even at the same pulse fluence the amount of energy incident on the PI surface would be lower, resulting in less ejection and therefore, no clear 'separation' of LIG along a line. Control over the distribution of LIG across a line therefore requires control over the amount of incident energy on the PI, to prevent ejection of the LIG formed.

To further investigate the impact of LIG line distribution on large area device fabrication, the next step for future work would be to compare the obtained observations to write large area patterns. To do so the proposed future work would also include the investigation of additional process parameters such as line overlap and hatch patterning. This work would be supported by SEM and Raman studies, followed by optimisation for different applications to showcase the impact of this study.

CONCLUSION

In this paper, the results of an investigation into the effect of fs pulse fluence and scanning speed on the distribution of LIG in scanned lines were presented. At high fluences (above 0.0832 Jcm^{-2}) and relatively low speeds (100 mms^{-1}), LIG along a single line was observed to become unevenly distributed and separated by a groove of ablated PI. Better understanding and control of this observed phenomenon, especially in relation to larger 2D LIG patterns is expected to improve the performance of LIG devices. It is envisaged that these results will contribute to the realisation of high performance, large area, multifunctional LIG/3D printed devices in the near future.

ACKNOWLEDGMENTS

This work was supported under the research collaboration agreement by Panasonic Factory Solutions Asia Pacific (PFSAP) and Singapore Centre for 3D Printing (SC3DP) (RCA-15/027).

REFERENCES

Andrea, Lamberti, Francesco, Perrucci, Matteo, Caprioli, Mara, Serrapede, Marco, Fontana, Stefano, Bianco, . . . Elena, Tresso. (2017). New insights on laser-induced graphene electrodes for flexible supercapacitors: tunable morphology and physical properties. *Nanotechnology, 28*(17), 174002.

Bolotin, K. I., Sikes, K. J., Jiang, Z., Klima, M., Fudenberg, G., Hone, J., . . . Stormer, H. L. (2008). Ultrahigh electron mobility in suspended graphene. *Solid State Communications, 146*(9), 351-355.

Chyan, Yieu, Ye, Ruquan, Li, Yilun, Singh, Swatantra Pratap, Arnusch, Christopher J., & Tour, James M. (2018). Laser-Induced Graphene by Multiple Lasing: Toward Electronics on Cloth, Paper, and Food. *ACS Nano*.

De, Sukanta, & Coleman, Jonathan N. (2010). Are There Fundamental Limitations on the Sheet Resistance and Transmittance of Thin Graphene Films? *ACS Nano, 4*(5), 2713-2720.

Duy, Luong Xuan, Peng, Zhiwei, Li, Yilun, Zhang, Jibo, Ji, Yongsung, & Tour, James M. (2018). Laser-induced graphene fibers. *Carbon, 126*, 472-479.

Ferrari, A. C., Meyer, J. C., Scardaci, V., Casiraghi, C., Lazzeri, M., Mauri, F., . . . Geim, A. K. (2006). Raman Spectrum of Graphene and Graphene Layers. *Physical Review Letters, 97*(18), 187401.

In, Jung Bin, Hsia, Ben, Yoo, Jae-Hyuck, Hyun, Seungmin, Carraro, Carlo, Maboudian, Roya, & Grigoropoulos, Costas P. (2015). Facile fabrication of flexible all solid-state micro-supercapacitor by direct laser writing of porous carbon in polyimide. *Carbon, 83*, 144-151.

James, Joseph, Murukeshan, Vadakke Matham, & Woh, Lye Sun. (2014). Integrated photoacoustic, ultrasound and fluorescence platform for diagnostic medical imaging-proof of concept study with a tissue mimicking phantom. *Biomedical Optics Express, 5*(7), 2135-2144.

Li, Yilun, Luong, Duy Xuan, Zhang, Jibo, Tarkunde, Yash R., Kittrell, Carter, Sargunaraj, Franklin, . . . Tour, James M. (2017). Laser-Induced Graphene in Controlled Atmospheres: From Superhydrophilic to Superhydrophobic Surfaces. *Advanced Materials, 29*(27), 1700496-n/a.

Lin, Jian, Peng, Zhiwei, Liu, Yuanyue, Ruiz-Zepeda, Francisco, Ye, Ruquan, Samuel, Errol L. G., . . . Tour, James M. (2014). Laser-induced porous graphene films from commercial polymers. *5*, 5714.

Lu, Yichen, Lyu, Hongming, Richardson, Andrew G., Lucas, Timothy H., & Kuzum, Duygu. (2016). Flexible Neural Electrode Array Based-on Porous Graphene for Cortical Microstimulation and Sensing. *6*, 33526.

Murukeshan, Vadakke Matham, Chua, Jeun Kee, Tan, Sia Kim, & Lin, Qun Yin. (2008). Nano-scale three dimensional surface relief features using single exposure counter-propagating multiple evanescent waves interference phenomenon. *Optics Express, 16*(18), 13857-13870.

Nakajima, Tomohiko, Nakamura, Takako, & Tsuchiya, Tetsuo. (2016). Flexible humidity sensors composed of graphite-like carbon micro-pinecone arrays. *RSC Advances, 6*(97), 95342-95348.

Novoselov, K. S., Geim, A. K., Morozov, S. V., Jiang, D., Zhang, Y., Dubonos, S. V., . . . Firsov, A. A. (2004). Electric Field Effect in Atomically Thin Carbon Films. *Science, 306*(5696), 666.

Schumann, M., Sauerbrey, R., & Smayling, M. C. (1991). Permanent increase of the electrical conductivity of polymers induced by ultraviolet laser radiation. *Applied Physics Letters, 58*(4), 428-430.

Sreekanth, KV, & Murukeshan, VM. (2010). Four beams surface plasmon interference nanoscale lithography for patterning of two-dimensional periodic features. *Journal of Vacuum Science & Technology B, Nanotechnology and Microelectronics: Materials, Processing, Measurement, and Phenomena, 28*(1), 128-130.

Sujatha, N., Murukeshan, V. M., Ong, L. S., & Seah, L. K. (2003). An all fiber optic system modeling for the gastrointestinal endoscopy: design concepts and fluorescent analysis. *Optics Communications, 219*(1), 71-79.

Zhao, Yang, Han, Qing, Cheng, Zhihua, Jiang, Lan, & Qu, Liangti. (2017). Integrated graphene systems by laser irradiation for advanced devices. *Nano Today, 12*, 14-30.